Heat Flux Manipulation with Engineered Thermal Materials

Supradeep Narayana and Yuki Sato

The Rowland Institute at Harvard, Harvard University, Cambridge, Massachusetts 02142, USA
(Received 6 March 2012; published 21 May 2012)

Utilizing a multilayered composite approach, we have designed and constructed a new class of artificial materials for thermal conduction. We show that an engineered material can be utilized to control the diffusive heat flow in ways inconceivable with naturally occurring materials. By shielding, concentrating, and inverting heat current, we experimentally demonstrate the unique potential and the utility of guiding heat flux.

Thermodynamics is a well-established discipline in science, and the concept of heat has been known for a long time. That often makes us forget how difficult it really is to manipulate heat flow in real life. Compared to the field of electric conduction armed with nonlinear solid-sate devices, heat conduction management is still in its infancy. The ability to precisely control heat current has significant implications beyond scientific curiosity, and can potentially lead to the development of thermal analogues of electronic transistors, rectifiers, and diodes. Here we show that an artificial material can be utilized to guide the heat flow in ways inconceivable with naturally occurring materials. We demonstrate this concept by engineering a new class of artificial material for thermal conduction and experimentally shielding, concentrating, and inverting the applied heat flux. The results constitute a vivid demonstration of extreme heat flux control with artificial materials and provide a conceptual insight that heat current, like electric and photonic current, should be viewed as a medium that can be manipulated, controlled, and processed.

The ability to manipulate the path of energy propagation is a trait that distinguishes artificial materials from ordinary materials. In a solid material supporting heat current, the properties induced from artificially arranged thermal conductivities can be counterintuitive. Although some theoretical work including the prediction of a thermal cloak has been carried out [1–3], such thermal "meta"-materials have, so far, not been investigated experimentally. We first discuss the shielding operation and then proceed to concentrating and inverting heat flux.

See Fig. 1(a). When a block of material is placed between a heat source and a sink, a uniform temperature gradient is established across the material. Heat current flows from left to right as indicated by the arrows. Figure 1(b) depicts the same block with a hollow cylindrical shield inserted at the center. Here we require the exterior region to exhibit the same temperature profile as Fig. 1(a) without the shield, while the interior region now needs to have no temperature gradient.

To gain control over the path of energy transport via thermal conduction, one needs to engineer an artificial material with prescribed anisotropy in its thermal conductivity. One of the most practical ways to introduce such anisotropy is to build a stacked composite from macroscopic layers of isotropic materials. Consider, for example, a composite made of alternating sheets of materials *A* and *B*. In a perpendicular direction, the two alternating conductances add in series, while they add in parallel in a transverse direction. Thus, the overall thermal conductivity of the effective medium becomes anisotropic, and the heat flux density vector changes direction as it propagates through the material. Building on this effect, one can design and assemble an artificial composite material that forces the heat flux to follow a particular path of interest.

A concentric layered structure consisting of alternating layers of materials *A* and *B* of different homogeneous isotropic thermal conductivities κ_A and κ_B is depicted in Fig. 2(a). For the host background material, we use a 5% agar-water block with thermal conductivity $\kappa_h \sim 0.56$ W/(mK) [4]. For the device to blend into the background thermally and not perturb the external field profile, the thermal resistance of the host material should be close to the reduced average of those of the two
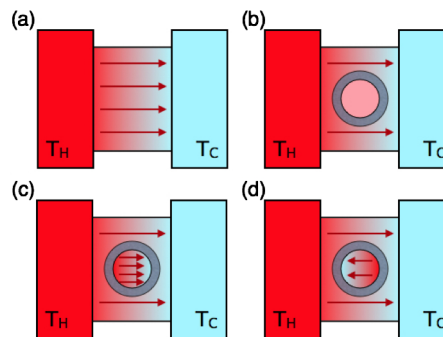

FIG. 1 (color online). (a) A block of material is placed between two heat baths. (b) Concept of thermal shielding by flux manipulation. (c) Concept of concentrating thermal flux. (d) Concept of inverting thermal flux.
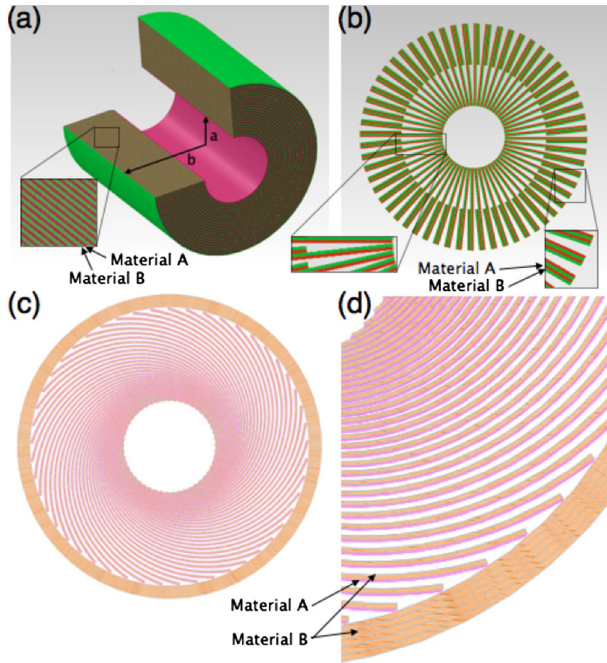
FIG. 2 (color online).   (a) Anisotropic thermal shield. The schematic shows a cut section for clarity. (b) Cross-sectional schematic for multilayered thermal concentrator. (c) Cross-sectional schematic for multilayered composite designed to invert the applied heat flux. (d) Close-up view of the inverter showing the constitutive materials.

materials employed in accordance with the effective medium approach [5,6]. The least perturbation is achieved when $\kappa_A \kappa_B \sim \kappa_h^2$. Although the effective wavelength of heat current considered here diverges, each layer thickness needs to be sufficiently small so that the composite effect dominates over properties of any individual layer while ensuring that the temperature variation across each layer remains small for fixed ∇T.

Based on the results of COMSOL Multiphysics finite element-based simulations, we have designed and constructed our cylindrical material from 40 alternating layers of 0.36 mm thick natural latex rubber film [$\kappa_A \approx$ 0.13 W/(mK)] and 0.38 mm thick silicone elastomers (Cho-Therm 1671) containing boron nitride particles to give $\kappa_B \approx 2.6$ W/(mK). The overall dimensions of the shield are roughly $a = 0.8$ cm, $b = 2.7$ cm, and 5 cm in length, and this material is cast in the agar-water block. The final host block has dimensions 8 cm (W), 5 cm (D), 18 cm (H), and the cylinder is flush with the host surface.

Before we present the results obtained with the shield characterized by artificially introduced anisotropy, we first discuss two isotropic materials. The first material for comparison is a hollow cylinder made of copper [$\kappa \approx$ 420 W/(mK)]. We have cast this material in agar-water block as described above and maintained the two sides of the block at 0 °C and 41 °C. This corresponds to an applied temperature gradient $\nabla T \approx 5.1$ K/cm. The simulated

results for the temperature profile and the heat flux lines are shown in Figs. 3(a) and 3(b). These should be compared with the experimentally measured temperature map shown in Fig. 3(c). The cross-sectional temperature profile is captured with a Flir E50 infrared camera. It is apparent that the presence of the shield completely alters the temperature gradient profile. The extremely high thermal conductivity of the copper attracts the heat flux lines and shunts them within the material. This keeps the inner region (as well as the region inside the annulus) free of thermal gradient. We measure the temperature gradient in the region $r < a$ to be 0.25 K/cm (5% of the applied gradient). The distortion of the external thermal profile can be assessed by the angle of isothermal lines. At the greatest point of perturbation (a point at the circumference of the copper block, 45° to the horizontal with respect to the shield center), we measure the isotherms to be at +43° where the direction of unperturbed isotherms is defined to be 0°.

The second material for comparison is a hollow cylinder made of polyurethane [$\kappa \approx 0.03$ W/(mK)]. The simulated results for the temperature map and the heat flux lines are
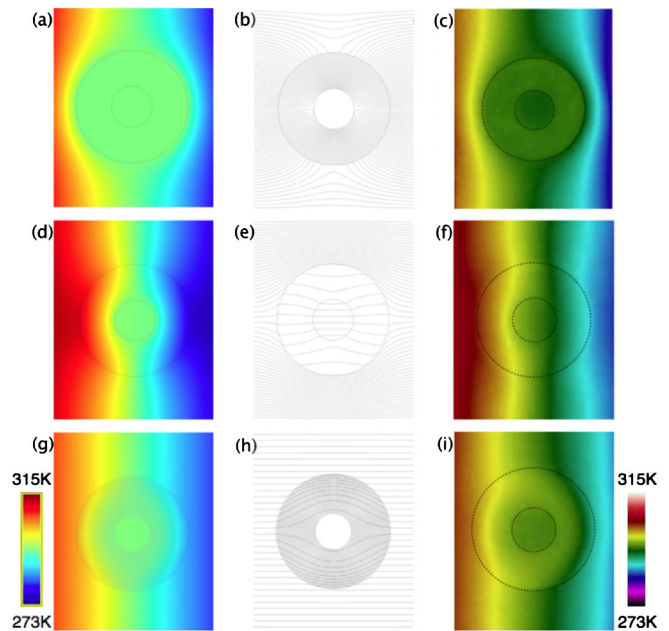

FIG. 3 (color online).   (a) Simulated temperature profile for a hollow copper cylinder placed in agar-water block. (b) Simulated heat flux lines. (c) Experimentally measured temperature map for the copper case. (d) Simulated temperature profile for a hollow polyurethane cylinder placed in agar-water block. (e) Simulated heat flux lines. (f) Experimentally measured temperature map for the polyurethane case. (g) Simulated temperature profile for a multilayered shield placed in agar-water block. (h) Simulated heat flux lines. (i) Experimentally measured temperature map for the reported shield. For the experimental data, dotted lines outline the inner and outer radii of shield materials. Left and right bars show the contrast scales for simulation and experimental images, respectively.

shown in Figs. 3(d) and 3(e), and they should be compared with the measured thermal profile of Fig. 3(f). Although polyurethane is often used for thermal insulation in various applications, its thermal conductivity is not quite low enough to completely shield the thermal gradient. We measure $\nabla T \approx 3.5$ K/cm ($\sim 70\%$ of the applied gradient) in the region $r < a$. The measured isotherm distortion at the same location of greatest perturbation as described above is $-15°$.

Finally, we present the results obtained with the layered composite material. The simulated temperature and the flux lines are shown in Figs. 3(g) and 3(h). The simulation shows the designed properties of the material: no distortion outside with no gradient inside with all the bending contained within the material. We show the experimental data in Fig. 3(i), which exhibits remarkable similarity to the simulated temperature plot. We measure $\nabla T \approx 0.38$ K/cm in the region $r < a$ ($\sim 7\%$ of the applied gradient). This inner thermal shielding is as efficient as that provided by a copper cylinder (although the individual thermal conductivities of constitutive elements are lower than that of copper by at least 2 orders of magnitude) and more effective than the more insulating polyurethane shield by an order of magnitude. This is made possible by the approach of rerouting the heat flow path within the material away from the region of interest unlike, for example, the polyurethane case where the idea is to simply put an insulating object in the path and hope to block some of the heat flux. What is just as striking here is that the temperature gradient outside the cylinder is hardly distorted unlike the two isotropic material cases above. We measure the isotherm distortion at the point of greatest perturbation to be $-1°$.

One of the practical strengths of material engineering lies with its inherent design flexibility. For example, with the ability to manipulate the heat flow with artificially introduced anisotropy, it becomes reasonable to wonder if the heat flux can be guided and concentrated for energy harnessing as depicted in Fig. 1(c). To explore such properties experimentally, we have constructed a hollow cylindrical device depicted in Fig. 2(b). We have configured the latex film and the elastomer as 240 azimuthally alternating layers here to achieve the high degree of anisotropy required for flux concentration. We have then cast this material in an agar-water block as before and applied the same temperature gradient across it.

We first show the simulated temperature map and heat flux lines in Figs. 4(a) and 4(b). The concentrator compresses the thermal flux of the annulus into a smaller inner volume such that the energy density in that region is considerably enhanced while remaining uniform. In Fig. 4(c), we show the experimentally obtained thermal image of the actual device. One can clearly see the prominent bending of the isothermal lines within the composite material in a direction opposite to the case of shielding discussed earlier, which increases the temperature gradient
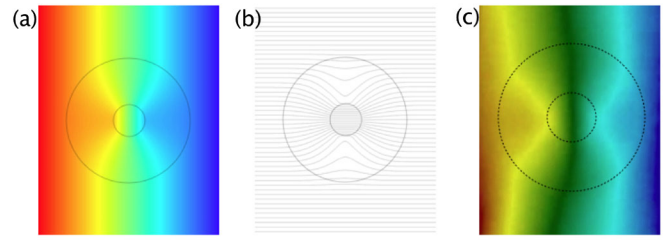

FIG. 4 (color online). (a) Simulated temperature profile for a concentrator placed in agar-water block. (b) Simulated heat flux lines. (c) Experimentally measured temperature map for the reported concentrator. Temperature scales are the same as those used in Fig. 3. We note the existence of the left-right asymmetry in the temperature profile in the experimental data and speculate that it may be due to the unequal layering of the materials employed.

and thus the overall heat flow in the inner agar region without affecting the exterior heat profile. We find that this particular concentrator increases the heat flux by 44% in the region $r < a$. Although the optimization of flux amplification was beyond the scope of this experiment, this type of thermal guiding may find applications in devices such as solar cells where high energy density with uniform distribution plays an important role.

Finally, we discuss a thermal inverter, whose idea is depicted in Fig. 1(d). What we report here is that the hollow cylindrical material can be made artificially with engineered properties such that now the heat current flows from right to left in the inner region without affecting the exterior heat current, which continues to flow from left to right. The geometrical pattern for the spatially varying thermal conductivity required for flux inversion is obtained following the transformation media concept developed for the rotation of electromagnetic waves with metamaterials [7–9]. In the absence of additional heat sources, the steady-state conduction equation can be written as $\nabla \cdot (\kappa \nabla T) = 0$. The coordinate transformation approach is applicable as the conduction equation is form invariant under such transformation [1,3,10–13] and provides a guideline for the design parameters to achieve extreme flux manipulation. For the rotational coordinate transformation: $r' = r$, $\theta' = \theta + g(r)$, where $g(b) = 0$, $g(a) = \theta_0$, and a and b are the inner and outer radii of the device, the geometry for the layered material can be expressed by a differential equation [7–9,14]: $rd\theta/dr = -(\sqrt{t^2 + 4} + t)/2$, where $t = \theta_0/\ln(b/a)$.

The cross-sectional view of the hollow cylindrical structure that we have assembled is schematically represented in Fig. 2(c), and a close-up view is shown in Fig. 2(d). The device that is concentric and fanlike at the same time consists of alternating layers of two isotropic materials with an overall bend in a spiral manner as determined by geometric transforms discussed above. Material A is a 0.13 mm thick copper sheet with $\kappa_A \approx 403$ W/(mK). Material B is a 0.38 mm thick polyurethane sheet with
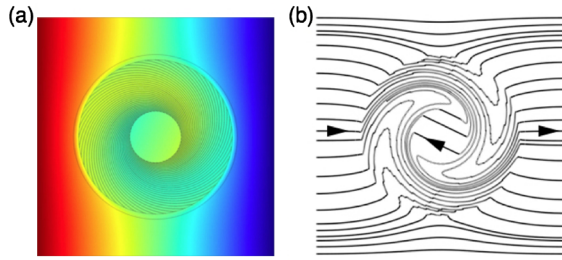
FIG. 5 (color online). (a) Simulated temperature profile for the reported device. (b) Simulated heat flux lines. The device's inner structures are not shown for the flux density plot for clarity. Arrows are guides to the eye to indicate flux direction.
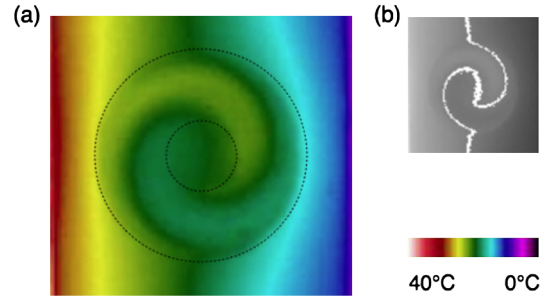

FIG. 6 (color online). (a) Experimentally measured thermal image showing the rotation of thermal gradient. Dotted lines outline the inner and outer diameters of the reported material. (b) Isothermal line for 20.3–20.7 °C.

$\kappa_B \approx 0.22$ W/(mK). There are 96 alternating layers total, and the structure is housed in 5 layers of the same polyurethane sheet. The overall dimensions are 6.4 cm (OD), 2 cm (ID), and 5 cm (H), and this object is cast in a host material of agar-water block.

Figure 5(a) shows the simulated temperature map for the artificial material described above. The isothermal regions rotate in a spiral manner within the composite material in such a way that the thermal gradient changes its sign in the inner region. The simulated heat flux pattern is shown in Fig. 5(b), which reveals the rotation of the heat flux vector. The rotation angle based on the employed spatial geometry and the materials' physical dimensions and their thermal properties is $\approx 204°$. This particular angle is chosen here so that the experimentally observed rotation angle, which is always less than the ideal simulation result, ends up as full inversion (i.e., 180°). The loss of $|\nabla T|$ in the inner region compared to the case without the hollow cylindrical device is $\approx 48\%$.

We show the experimentally observed thermal image in Fig. 6(a). Rotation of the isotherms is clearly visible from their swirling patterns resembling the simulated result of Fig. 5(a). We highlight the isothermal line representing the temperature range 20.3–20.7 °C in Fig. 6(b), which demonstrates the nontrivial inversion of the thermal gradient in the inner region with respect to the exterior. The observed rotation angle is $\approx 179°$. For the externally applied temperature gradient $\nabla T \approx -4.3$ K/cm (from left to right), we observe $\nabla T \approx +1.7$ K/cm in the inner region, confirming the heat flow reversal. For the same external ∇T applied in the experiment, the temperature gradient in the inner region expected from simulation is $\nabla T \approx +2.2$ K/cm. If a conventional isotropic material is used for the situation depicted in Fig. 1(d), the reversal of temperature gradient becomes unrealizable. For the heat current flowing from left to right, the heat flux vector will never pick up a component pointing from right to left within the material, let alone invert in the inner region. It is the engineered thermal properties of the artificial material here that make such a phenomenon observable.

For the shield and the concentrator, constituent elements give the reduced thermal conductivity that is close to the background with $\kappa_A \kappa_B \sim \kappa_h^2$. However, in the inverter case, the difference between the thermal conductivities of the copper sheets and the background is much larger than it is for the polyurethane sheets and the host. The overall object, therefore, tends to appear more conductive to the background, resulting in finite distortion of the exterior temperature profile. We note that if the flux-guiding devices are engineered with materials with temperature-dependent thermal conductivities [15], one can turn the designed functionalities on and off with a temperature change in the environment. Such thermal devices may provide the nonlinearity necessary as building blocks for thermal circuits [16].

In summary, utilizing the multilayered composite approach, we have designed and constructed a new class of artificial material for a diffusive energy transport of thermal conduction. By employing only isotropic elements but prescribing particular spatial patterns, we have introduced the anisotropy required for thermal guiding. By shielding, concentrating, and inverting heat current, we have experimentally demonstrated some of the potential and the utility of guiding heat flux. Artificially engineered thermal materials can yield characteristics that go far beyond those obtainable with conventional media, and such materials should lead to unprecedented heat flux control and novel applications.

[1] C. Z. Fan, Y. Gao, and J. P. Huang, Appl. Phys. Lett. **92**, 251907 (2008).
[2] T. Chen, C. N. Weng, and J. S. Chen, Appl. Phys. Lett. **93**, 114103 (2008).
[3] J. Y. Li, Y. Gao, and J. P. Huang, J. Appl. Phys. **108**, 074504 (2010).
[4] M. Zhang, Z. Che, J. Chen, H. Zhao, L. Yang, Z. Zhong, and J. Lu, J. Chem. Eng. Data **56**, 859 (2011).

[5] D. J. Bergman, Phys. Rep. **43**, 377 (1978).

[6] D. J. Bergman, Phys. Rev. B **19**, 2359 (1979).

[7] H. Chen and C. T. Chan, Appl. Phys. Lett. **90**, 241105 (2007).

[8] H. Chen and C. T. Chan, Phys. Rev. B **78**, 054204 (2008).

[9] H. Chen, B. Hou, S. Chen, X. Ao, W. Wen, and C. T. Chan, Phys. Rev. Lett. **102**, 183903 (2009).

[10] G. W. Milton, M. Briane, and J. R. Willis, New J. Phys. **8**, 248 (2006).

[11] S. Guenneau, C. Amra, and D. Veynante, Opt. Express **20**, 8207 (2012).

[12] A. Greenleaf, M. Lassas, and G. Uhlmann, Math. Res. Lett. **10**, 685 (2003), http://www.mathjournals.org/mrl/2003-010-005/2003-010-005-011.pdf.

[13] A. Greenleaf, M. Lassas, and G. Uhlmann, Physiol. Meas. **24**, 413 (2003).

[14] H. Chen, J. Yang, J. Zi, and C. T. Chan, Europhys. Lett. **85**, 24004 (2009).

[15] K. Berggold, M. Kriener, C. Zobel, A. Reichl, M. Reuther, R. Müller, A. Freimuth, and T. Lorenz, Phys. Rev. B **72**, 155116 (2005).

[16] N. Li, J. Ren, L. Wang, G. Zhang, P. Hanggi, and B. Li, arXiv:1108.6120v3 [Rev. Mod. Phys (to be published)].